Incorporation of 3T3-L1 Cells To Mimic Bioaccumulation in a Microscale Cell Culture Analog Device for Toxicity Studies†

Kwanchanok Viravaidya and Michael L. Shuler*

School of Chemical and Biomolecular Engineering, Cornell University, Ithaca, New York 14850-5201

Deficiencies in the early ADMET (absorption, distribution, metabolism, elimination, and toxicity) information on drug candidates extract a significant economic penalty on pharmaceutical firms. We have developed a microscale cell culture analog (μCCA) device that can potentially provide better, faster, and more efficient prediction of human and animal responses to a wide range of chemicals. The system described in this paper is a simple four-chamber μCCA ("lung"−"liver"−"fat"−"other tissue") designed on the basis of a physiologically based pharmacokinetics (PBPK) model of a rat. Cultures of L2, HepG2/C3A, and differentiated 3T3-L1 adipocytes were selected to mimic the key functions of the lung, liver, and fat compartments, respectively. Here, we have demonstrated the application of the μCCA system to study bioaccumulation, distribution, and toxicity of selected compounds. Results from the bioaccumulation study reveal that hydrophobic compounds such as fluoranthene preferentially accumulated in the fat chamber. Only a small amount of fluoranthene was observed in the liver and lung chambers. In addition, the presence of the differentiated 3T3-L1 adipocytes in the μCCA device significantly reduced naphthalene and naphthoquinone-induced glutathione (GSH) depletion. These findings suggest the potential utilization of the μCCA system to assess ADMET characteristics of the compound of interest prior to animal or human trials.

Introduction

Early determination of ADMET (absorption, distribution, metabolism, elimination, and toxicity) profiles of drug candidates is crucial in the drug discovery process, because deficiencies in ADMET characteristics are the leading cause of attrition during drug development (*1*). The traditional in vitro testing or cell-based assays cannot provide accurate information about ADMET of potential drugs due to its unrealistic setting (e.g., static condition and no interaction between cells, etc.) that does not mimic physiological conditions. Moreover, the impact of absorption of the compounds into fat tissue is usually neglected in these in vitro studies. Information from animal studies of the drug candidates is required by the Food and Drug Administration (FDA) to proceed to human clinical trials (*2*). These experiments are expensive, lengthy, and subject to ethical issues. Therefore, a system that can provide faster and more efficient screening of drug compounds should lead to more effective use of animals, provide human surrogates to facilitate cross-species extrapolation, and improve the success rate in the drug discovery process.

We have developed an in vitro model that can inexpensively and realistically test the response of humans and animals to various chemicals. This system is called a microscale cell culture analog (μCCA) and is designed on the basis of physiologically based pharmacokinetic (PBPK) models (*3*, *4*). A PBPK model is a mathematical representation of the body as interconnected organ compartments (*5*, *6*). The microfabricated device consists of a fluidic network of channels and chambers etched in a 2.5 cm × 2.5 cm silicon chip. Each chamber contains the culture of mammalian cells representing key functions of that particular "organ" and is interconnected by circulating culture medium to simulate the circulatory system (*3*). Microscale dimension provides a number of advantages, especially, a better mimic of the appropriate physiological scale.

We have designed and fabricated a four-chamber ("lung"−"liver"−"fat"−"other tissue") μCCA device. In the previous study, we have described the application of a simple two-cell μCCA system for a proof-of-concept study using naphthalene as a model toxicant (*4*). Two chambers (lung and liver) contain living cells, while the other tissue (or rapidly perfused tissues) and fat compartments (or slowly perfused tissues) have no cells but mimic the distribution of fluid. We have found that naphthalene metabolites formed in the liver compartment circulate to the lung compartment and deplete glutathione (GSH) in lung cells (L2). GSH is a tripeptide important in the cellular defense mechanism, and its depletion is associated with increased sensitivity to xenobiotic chemicals and toxicity. Also, 1,2-naphthalenediol and 1,2-naphthoquinone are the reactive circulating metabolites responsible for GSH depletion in lung cells. Although this simple two-cell system is a useful tool to probe naphtha-

* Corresponding author. Telephone: (607) 255-7577. FAX: (607) 255-9166. E-mail: mls@cheme.cornell.edu.

† List of abbreviations: mCCA, microscale cell culture analogue; PBPK, physiologically based pharmacokinetics; GSH, glutathione; ADMET, absorption, distribution, metabolism, elimination, and toxicity; DMEM, Dulbecco's modified eagle medium; F12, F-12 nutrient mixture (Ham); FBS, fetal bovine serum; MCB, monochlorobimane; L2, rat lung Type II epithelial cells; HepG2/C3A or C3A, human hepatocyte cell line; 3T3-L1, transformed rodent preadipocyte cell line.

10.1021/bp034238d CCC: $27.50
Published on Web 12/12/2003

lene toxicity and is satisfactory for a proof-of-concept experiment, it is still somewhat unrealistic and of limited utility.

Understanding the dynamic process of bioaccumulation is very important in predicting the responses of humans and animals to chemical or pharmaceutical exposure. Bioaccumulation has become a critical consideration in the regulation of chemicals (*7*) and is important in understanding the ADMET characteristic of the drug candidates. The lipophilic compounds can accumulate in the lipid component of the adipose tissue in humans and animals faster than they are metabolized or excreted, which increases the concentration of those particular compounds in the body over time. To address this issue, we have incorporated the fat tissue into the μCCA system to provide a bioaccumulation site for hydrophobic compounds. This three-cell system allows the bioaccumulation, distribution, metabolism, and toxicity studies to be performed all on the same device.

Several cell models to represent the fat chamber in the μCCA system have been considered. Fat tissue or adipose tissue consists of one-third to two-thirds adipocytes (primary fat cells) (*8*). However, this cell type is difficult to maintain in culture and poses a problem with adherence because of its buoyancy. Thus, primary adipocytes are not suitable for the μCCA system, which requires cells to attach to the surface. Transformed rodent preadipocyte cell lines have been considered as an alternative. These cell lines can differentiate into mature adipocytes when exposed to the right stimuli (*9*, *10*), and remain attach to the surface, satisfying the restriction of the μCCA system. Among all the preadipocyte cell lines we tested previously, differentiated 3T3-L1 adipocytes have been shown to yield the highest intracellular lipid content and accumulate the highest level of naphthalene (*11*). The ability of the differentiated 3T3-L1 adipocytes to accumulate naphthalene is also comparable to that of primary adipocytes. Therefore, we have selected the differentiated 3T3-L1 adipocytes to mimic the accumulation of the tested compound in the fat chamber.

In this paper, we describe the application of a three-cell system (lung−liver−fat) to study bioaccumulation, distribution, and toxicity. GSH depletion is used as an indicator of the naphthalene- and naphthoquinone-induced toxicity. The results obtained from the three-cell system are compared to the results from the previous two-cell-type system (*4*) to assess the modification in dynamic response due to the presence of 3T3-L1 adipocytes.

Materials and Methods

Materials. All medium components including DMEM/F12 (1:1), DMEM with high glucose content, fetal bovine serum (FBS), penicillin, streptomycin, pyruvate, and phosphate buffer saline (PBS) were purchased from Life Technologies, Inc., (Rockville, MD). Other reagents such as dexamethasone, indomethacin, human insulin, Oil Red O, triolein (C18:1, [cis]-9), 2-propanol, poly-D-lysine, naphthalene, naphthoquinone, and fluoranthene were obtained from Sigma (St. Louis, MO). Matrigel was acquired through Collaborative Biomedical Products (Bedford, MA). Fluorescence stains, such as calcein and monochlorobimane (MCB), and Amplex Red hydrogen peroxide assay kit (A-22188) were both purchased from Molecular Probes (Eugene, OR).

***μ*CCA Fabrication and Device Assembly.** The silicon μCCA device was fabricated using the standard lithography technique, as described elsewhere (*3*, *12*). The fabrication was done in a two-step etching process. The first step was a 20 μm etch for the lung and liver chambers, and the second step was a 100 μm etch for the fat, other tissue, and all connecting channels. Details of μCCA assembly are provided by Sin et al. (*3*, *12*). A description of the microfluidics of the four-compartment system is described elsewhere (*4*). After the μCCA device was assembled, a color dye was pumped through using an external peristaltic pump (205S; Watson-Marlow, Wilmington, MA) at 2 μL/min flow rate to visualize fluid flow and leakage in the system.

Cell Culture. L2 (rat lung Type II epithelial cells), HepG2/C3A (human hepatocytes), and 3T3-L1 cells were obtained from American Type Culture Collection (ATCC, Bethesda, MD). L2 and HepG2/C3A cell lines were maintained in DMEM/F12 tissue culture medium supplemented with 10% FBS, 50 units/mL penicillin, and 50 μg/mL streptomycin. Pyruvate was added to the medium for HepG2/C3A. 3T3-L1 cells were maintained in the preadipose condition using preadipocyte medium which consists of DMEM medium supplemented with 10% FBS, 50 units/mL penicillin, and 50 μg/mL streptomycin.

To initiate adipocyte differentiation, cells were allowed to reach 2 days postconfluence. 3T3-L1 cells were differentiated with the differentiation medium (preadipocyte medium containing 125 μM indomethacin, 1 μM dexamethasone, and 5 μg/mL insulin) for 48 h. Then, the differentiation medium was replaced with the adipocyte medium or the preadipocyte medium supplemented with 5 μg/mL insulin (*11*).

***μ*CCA Cells on a Chip.** A μCCA chip was initially coated with poly-D-lysine at 10 μg/cm^2. A silicone gasket (GRACE-BIO) was applied to the surface of the silicon chip providing a hydrophobic barrier to confine cell suspensions to the proper compartments and prevent cross-contamination of compartments. The lung, liver, and fat chambers were then coated with Matrigel at 100 μg/cm^2 density, according to the manufacturer's instructions. Because 3T3-L1 cells require longer incubation time to accumulate intracellular lipid, initially, only 3T3-L1 cells were plated on the chip. A 60 μL aliquot of 3T3-L1 cell solution was added to the fat chamber. Cells were allowed to attach for 4−6 h before 5 mL of preadipocyte medium was added. After 2 day postconfluency, 3T3-L1 adipocytes were differentiated according to the above procedure. Before plating L2 and HepG2/C3A cells on the μCCA device, the lung and liver, but not the fat, chambers were allowed to dry completely. A 40 μL aliquot of L2 at 2×10^5 cells/mL was plated into the lung chamber, whereas 40 μL of HepG2/C3A at 1×10^6 cells/mL was seeded into the liver chamber. A 60 μL aliquot of adipocyte medium was added to the fat chamber. The chips were then incubated at 37 °C to let the cells attach. After 4 h, the silicone gasket was removed, and DMEM/F12 medium, supplemented with 10% FBS and 5 μg/mL insulin, was added to maintain the cells overnight.

***μ*CCA-Bioaccumulation Study.** Fluoranthene, a naturally fluorescent polycyclic aromatic hydrocabon, is used as a model compound. The assembled three-cell system device was connected to a 100 μL reservoir (debubbler) containing DMEM/F12 medium supplemented with 10% FBS and operated using a peristaltic pump at 2 μL/min flow rate at 37 °C in a humidified, 5% CO_2 atmosphere. The fluoranthene treated μCCA chips were dosed through the reservoir at the initial concentration of 300 μg/mL. To terminate the experiment, serum-free medium without phenol red was pumped into the system for 15 min to rinse the cells before acquiring fluorescence images.

***μ*CCA-Toxicity Study.** The viability of cells on the

μCCA chips was checked under the reflective microscope before and after the devices were assembled. Then, the assembled device containing cells was connected to a 100 μL reservoir (debubbler) and a peristaltic pump to provide recirculation at 2 μL/min. DMEM/F12 supplemented with 10% FBS was used as a blood surrogate. The system was operated at 37 °C in a humidified, 5% CO_2 atmosphere. In each set of experiment, three control devices [control indicates the μCCA system that was not exposed to naphthalene or naphthoquinone] were run in parallel to three chemically treated devices.

In naphthalene toxicity studies, naphthalene was maintained at the saturation limit by addition of excess naphthalene to avoid losses due to naphthalene's high volatility. Naphthalene concentration was previously measured to be 50 μg/mL in the culture medium supplemented with 10% serum (*12*). To obtain time course data, multiple experiments were required as the addition of stain terminated that experiment. In the naphthoquinone toxicity study, μCCA chips were treated with various concentrations of naphthoquinone for 6 h. Naphthoquinone was dosed through a reservoir. At the end of each experiment, cells on the chip were stained with calcein (LIVE stain) and monochlorobimane (MCB; glutathione (GSH) stain) (*13*) by recirculating DMEM medium without phenol red containing 5 μM calcein and 80 μM MCB at 37 °C for 30 min. Later, DMEM medium without phenol red was fed into the system for 15 min to remove excess dye. Results are presented as a percentage of the control.

Fluorescence Microscopy and Image Analysis. Fluorescence images were acquired using an epifluorescence microscope (Metamorph) equipped with a 20× objective. Fluorescence of fluoranthene and MCB-GSH adduct was excited by light provided by a xenon lamp using a 10 nm band-pass filter centered at 360 nm in the light path and emitted through a 460 nm long-pass filter, while fluorescent calcein was excited at 483 nm excitation and 535 nm emission. Image analysis to obtain fluorescent intensity used Scion Image (Scion Corp., Frederick, MD).

Naphthoquinone Accumulation Study. 3T3-L1 adipocytes were differentiated for 20 days to reach maturity. The naphthoquinone accumulation study was carried out in 12-well tissue culture plates (Corning). Cells were incubated with various concentrations of naphthoquinone solution for 6 h. At the end of the experiment, the absorbance of the culture medium was measured at 250 nm. The amount of accumulated naphthoquinone was determined from the disappearance of naphthoquionone in the supernatant from adipocyte. To correct for background disappearance, each point value was subtracted from the disappearance of naphthoquinone in the control [the control experiments were the incubation of naphthoquinone in the absence of adipocytes to account for background disappearance of naphthoquinone]. The amount of lipid in the differentiated 3T3-L1 adipocytes was quantified as described previously (*11*). All the experiments were done in triplicate.

H_2O_2 Production from Naphthoquinone in the Presence of 3T3-L1 Adipocytes. 3T3-L1 adipocytes were also differentiated for 20 days before the experiment. This study was carried out in a 96-well tissue culture plate (Corning). The culture medium was removed, and the differentiated adipocytes were rinsed with PBS twice for complete removal of serum. Adipocytes were then incubated with various concentrations of naphthoquinone in DMEM (without phenol red) serum-free medium for 6 h. Hydrogen peroxide generated from naphthoquinone was quantified using an Amplex Red hydrogen peroxide assay, according to the manufacturer's instruction. The samples were read for absorbance at 560 nm. To correct for background absorbance, each point value was subtracted from the value of negative control.

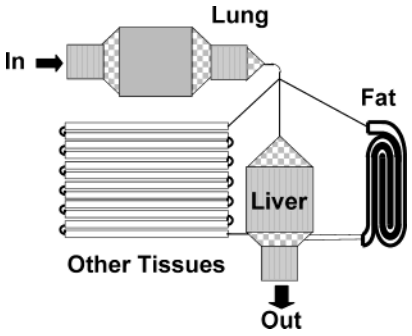

Figure 1. Schematic diagram of a four-chamber μCCA. The microfabricated device comprises two depths, 20 μm (depicted in gray) for the lung and liver chambers and 100 μm (depicted in white) for the other tissue, fat, and all channels. The dimensions of the chambers are as followed ($w \times l$): lung, 2 × 2; liver, 3.5 × 4.6; fat, 0.42 × 50.6; and other tissues, 0.4 × 109. Units are in millimeters.

Statistics. An unpaired Student's *t*-test was used for data analysis. Significant difference was defined at the 95% confidence level.

Results

Design and Microfluidics of a Four-Chamber μCCA. A four-chamber μCCA device is designed on the basis of the PBPK model of a 220 g rat (*14*, *15*) and constraints described in Sin et al. (*3*) In a four-chamber system, the fat compartment is separated from the other tissue to accurately mimic the accumulation dynamics of tested compounds in living organisms. The schematic diagram of a four-chamber μCCA is illustrated in Figure 1. The culture medium or blood surrogate, first entering the system through the inlet, passes through to the lung, after which 9, 25, and 66% of fluids go into the fat, liver, and other tissue chambers, respectively. The fluids from these three chambers are then combined before being pumped out through the outlet and circulated back to the inlet.

Obtaining a complete seal between Plexiglas and the μCCA chip is important, as small gaps between them can lead to leakage and eventually deplete the fluid from the system. Color dye was pumped through the assembled device to visualize the flow. No leaking was observed (Figure 2).

Cells on a Chip. Culturing three different cell types on a chip can be challenging, because these cells grow at different rates, and most importantly, the 3T3-L1 adipocyte cell line requires prolong incubation time to differentiate and accumulate intracellular lipid. Thus, 3T3-L1 cells need to be plated in the fat chamber first. Once 3T3-L1 adipocytes are differentiated, L2 and C3A cells can be cultured on the μCCA chip. It is important to have the lung and liver chambers completely dry before inoculation; otherwise, cell suspension would be diluted and cross-contaminate other chambers.

We have determined the ability of the μCCA device to maintain cell cultures under flow environment. The fluid in the μCCA system was recirculated for 6 h after all cells reached the desired level of confluency and the device was assembled. At the end of the experiment, cells on the chip were stained with LIVE stain (calcein) to visualize cell viability and attachment. As shown in

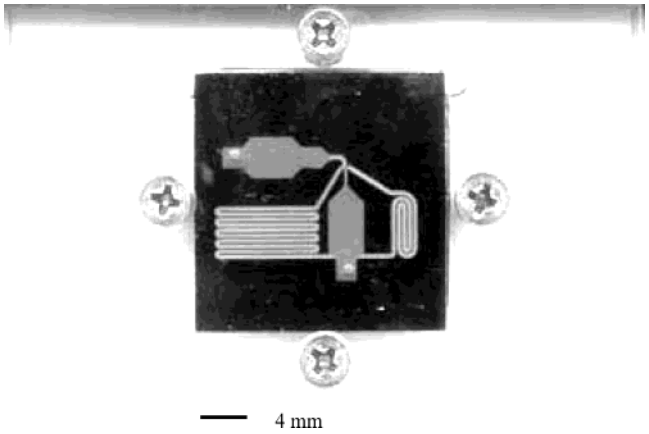

Figure 2. Color dye pumped through the assembled μCCA system to visualize the flow distribution and leakage in the system.

Figure 3, cells in each chamber were viable, confluent and remained attached at the end of experiment. The enlarged image of 3T3-L1 adipocytes shows evidence of intracellular lipid droplets. Some of the adipocytes around the edge detached from the wall of the fat chamber. Nonetheless, the majority of differentiated adipocytes were still intact upon circulation for 6 h.

***μ*CCA-Bioaccumulation Study.** Fluoranthene, a model compound in this study, is a representative of polycyclic aromatic hydrocarbons with high hydrophobicity (log $K_{ow} = 5.19$) (*16*). It provides strong blue fluorescence emission, which allows the use of fluorescence microscopy to directly determine the amount of accumulated fluoranthene in each chamber without taking the system apart.

The amount of fluoranthene in each chamber in the μCCA system was determined according to its fluorescence intensity at various time points (Figure 4). Before acquiring fluorescence images, cells in each chamber were checked on their confluency under the reflective microscope to ensure that the low fluorescence intensity was the result of less fluoranthene accumulated, not the result of cells detached from the surface. The majority of fluoranthene was accumulated in the fat chamber as early as 2 h and continued to increase until 6 h ($p < 0.001$). Much less fluoranthene accumulated in both the lung and liver chambers, although the level of fluoranthene in the liver was slightly higher than in the lung.

***μ*CCA-Naphthalene Toxicity.** To study the effect of addition of fat tissue on naphthalene toxicity, a three-cell μCCA system (with differentiated 3T3-L1 adipocytes) was challenged with naphthalene-saturated medium, similarly to the two-cell system (without 3T3-L1 adipocytes). The biomarker for toxicity is glutathione (GSH) depletion. Intracellular GSH is determined using monochlorobimane (MCB). MCB, a nonfluorescent bimane, develops strong blue fluorescence upon binding to thiol in the presence of glutathione-S-transferases (GST). The fluorescence intensity of this adduct is directly proportional to GSH in the cells (*17*).

Figure 5 presents the comparison of GSH levels in L2 and C3A cells between the μCCA system with 3T3-L1 adipocytes (three-cell system) and the system without 3T3-L1 adipocytes (two-cell system) upon naphthalene dosing. Both systems had the fat chamber, but only in the three-cell system were 3T3-L1 adipocytes added. The level of GSH in L2 cells in both systems decreased in a time-dependent manner (Figure 5A). However, the intracellular GSH of L2 cells in the μCCA system without 3T3-L1 adipocytes decreased more (GSH level at 60% of the control) than that of L2 cells in the system with 3T3-L1 adipocytes (80% of the control) at the end of 6 h ($p < 0.05$). In the liver chamber, GSH of C3A cells in the system with 3T3-L1 adipocytes remained high through the experiment (95−100% of the control), while the GSH

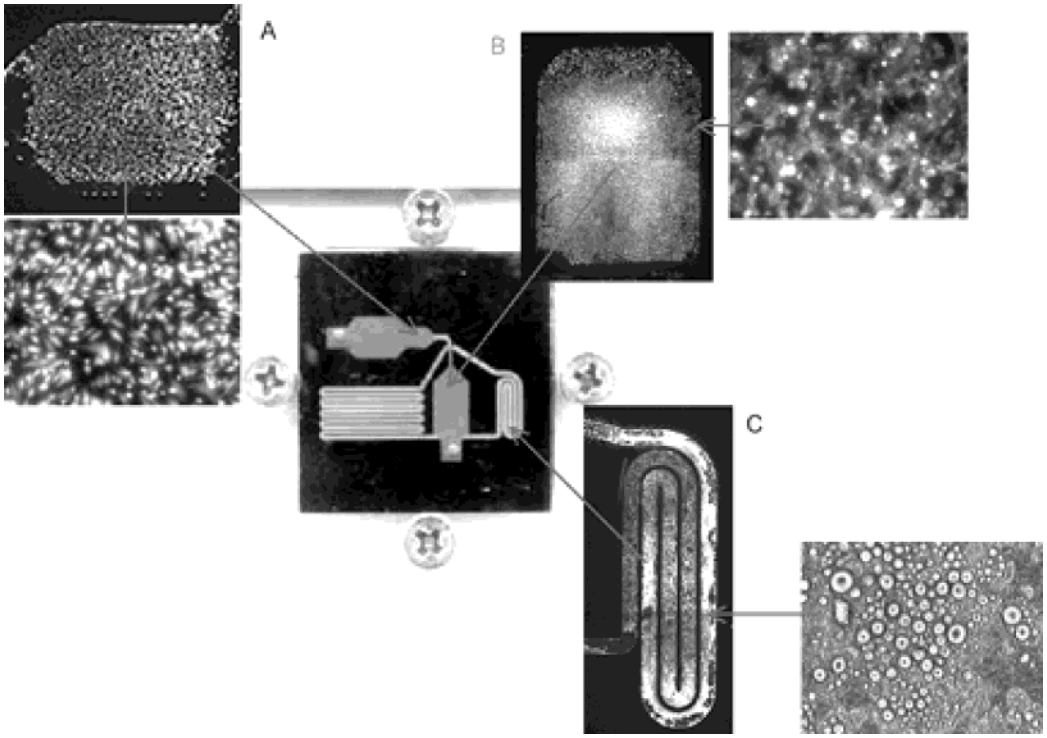

Figure 3. Cells on the μCCA chip after being in circulation for 6 h and stained with LIVE stain to visualize cell viability and attachment. A indicates L2 cells in the lung chamber and an enlarged image of L2 cells. B indicates HepG2/C3A in the liver chamber and enlarged image of C3A cells. C indicates the differentiated 3T3-L1 in the fat chamber. Cells in the chamber are 4· magnification and enlarged images are 20· magnification.

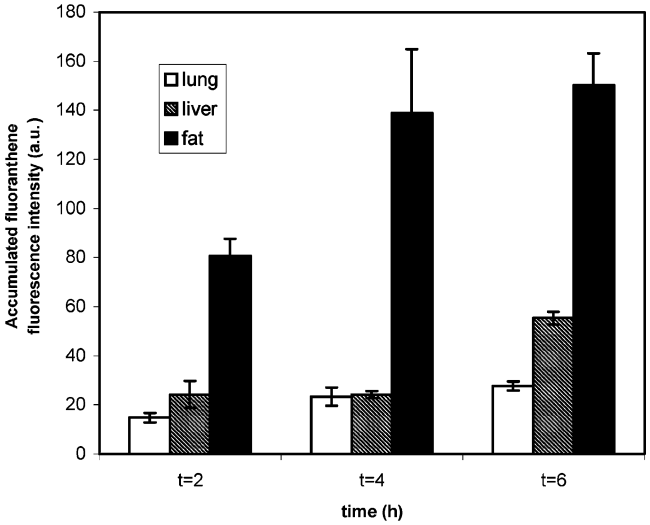

Figure 4. Amount of fluoranthene accumulated in the lung, liver, and fat chambers in the μCCA system was measured on the basis of its fluorescent intensity (au = arbitrary unit) at various time points.

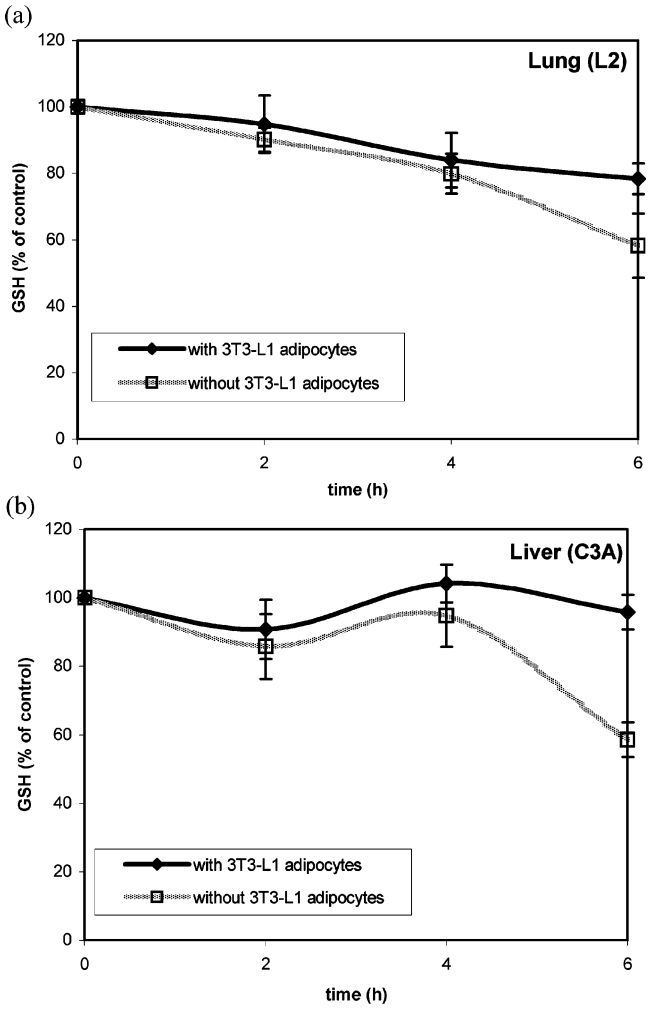

Figure 5. μCCA experiment-naphthalene toxicity study. The levels of glutathione (GSH) in (A) L2 cells and (B) HepG2/C3A cells are compared between naphthalene-treated three-cell (with addition of 3T3-L1 adipocytes) and two-cell (without 3T3-L1 adipocytes) μCCA devices (n = 3). The result is presented as a percentage of the control where the control is the μCCA system that was not exposed to naphthalene.

level in C3A cells in the system without 3T3-L1 adipocytes dropped to about 60% of GSH in C3A control

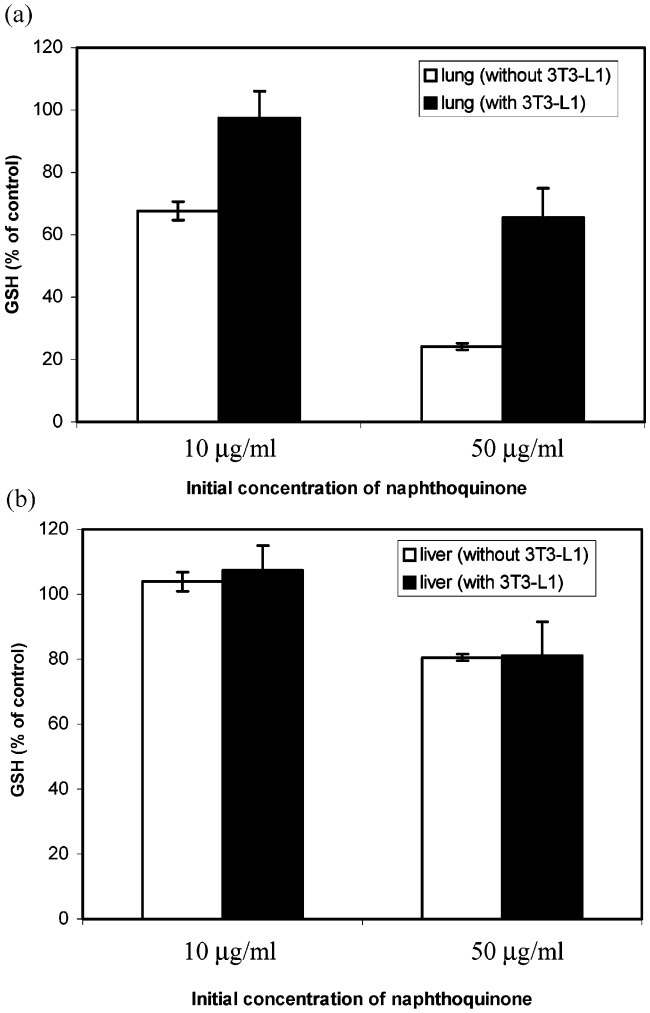

Figure 6. μCCA experiment—naphthoquinone toxicity study. The levels of glutathione (GSH) in (A) L2 cells and (B) HepG2/C3A cells are compared between naphthoquinone-treated three-cell (with addition of 3T3-L1 adipocytes) and two-cell (without 3T3-L1 adipocytes) μCCA devices (n = 3). The result is presented as a percentage of the control where the control is the μCCA system that was not exposed to naphthoquinone.

cultures at the end of 6 h ($p < 0.001$). Nonetheless, the qualitative trends of naphthalene-induced GSH depletion in L2 and C3A are the same in the μCCA systems both with and without 3T3-L1 adipocytes, but the presence of 3T3-L1 adipocytes reduces the quantitative level of response.

***μ*CCA-Naphthoquinone Toxicity.** Naphthoquinone has been identified as the most toxic metabolite derived from naphthalene metabolism and one of the metabolites responsible for naphthalene-induced GSH depletion in L2 cells (*4*). The three-cell μCCA system (with 3T3-L1 adipocytes) was treated with two concentrations of naphthoquinone, 10 and 50 μg/mL for 6 h. The results obtained from the three-cell system were compared with results from the two-cell system (without 3T3-L1 adipocytes) (Figure 6).

Although, the level of GSH in L2 cells in both systems decreased with increasing concentration of naphthoquinone, the GSH level of the L2 cells in the system without 3T3-L1 adipocytes decreased much more than that of L2 cells in the system with 3T3-L1 adipocytes ($p < 0.005$), and the differences in GSH depletion was more pronounced at higher concentration of naphthoquinone (30% vs 40%). Surprisingly, there was no significant difference between GSH levels in C3A cells in both

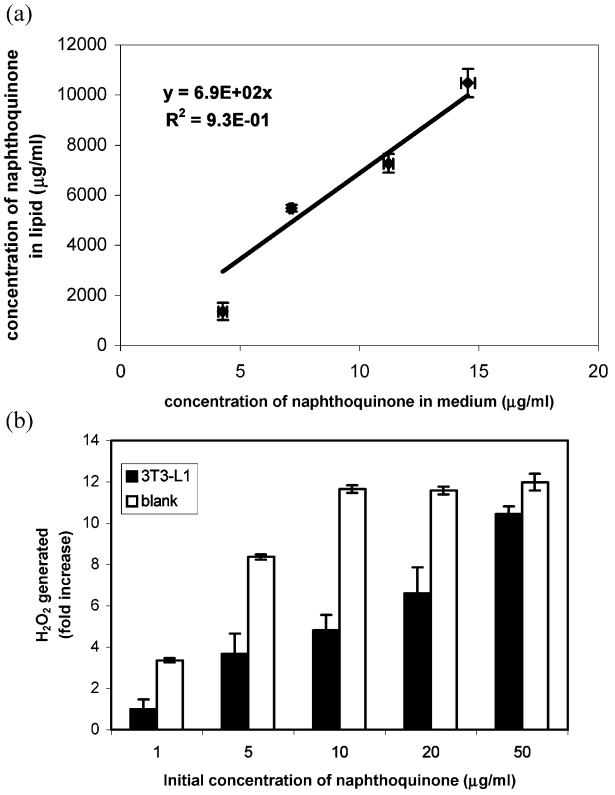

Figure 7. Differentiated 3T3-L1 adipocytes treated with various concentrations of naphthoquinone for 6 h to determine (A) the amount of naphthoquinone accumulated in 3T3-L1 adipocytes (n=3) and (B) the amount of H_2O_2 generated from naphthoquinone (n = 6). The intracellular lipid was converted from milligram of lipid to milliliter of lipid to satisfy the dimensionless nature of the partition coefficient. Hydrogen peroxide production is compared with the typical amount of H_2O_2 generated from naphthoquinone in culture medium without the presence of cells.

systems. Moreover, the reduction of the GSH level in C3A cells was always less than that of GSH in L2 cells treated at the same concentration of naphthoquinone.

Naphthoquinone Accumulation and H_2O_2 Disappearance in the Presence of 3T3-L1 Adipocytes. To investigate the possible causes of the differences in GSH response to naphthoquinone between the μCCA system with adipocytes and the system without adipocytes, the differentiated 3T3-L1 adipocytes were incubated with various concentrations of naphthoquinone for 6 h. At the end of the experiment, the amount of naphthoquinone accumulated into 3T3-L1 adipocytes and H_2O_2 production from naphthoquinone were determined. These measurements were taken independently.

The partitioning of naphthoquinone between culture medium and lipid in 3T3-L1 adipocytes was obtained (Figure 7A). The amount of accumulated naphthoquinone in adipocytes was initially determined as micrograms of naphthoquinone per milligram of lipid. The weight of lipid was later converted to lipid volume using 0.92 g/mL as a density of triglyceride (*18*), the majority lipid component in adipocytes. The conversion from lipid weight to lipid volume satisfies the dimensionless nature of the partition coefficient. The plot of naphthoquinone in the medium and in adipocytes is linear over the concentration range studied, and the slope yields the partition coefficient of 690. The log of the partition coefficient measured in our study (log $P_{\text{medium:adipocyte}}$ = 2.83) is reasonably closed to the estimated log of the octanol/water partition coefficient of 1,2-naphthoquinone (log K_{ow} = 2.11 [log K_{ow} of 1,2-naphthoquinone was estimated on the basis of the chemical structure using the SRC's LogKow program]). This finding indicates that naphthoquinone preferentially accumulated in the adipocytes. However, the accumulation of naphthoquinone in the adipocytes (11 $\pm$ 0.6 μg/(mg of lipid)) is still less than that of naphthalene (20 $\pm$ 2 μg/(mg of lipid)) at 6 h, probably because naphthoquinone is less hydrophobic.

H_2O_2 is produced through the redox cycle between naphthoquinone and naphthalenediol and is believed to cause cellular damage (*19*). The amount of H_2O_2 generated from naphthoquinone with and without the presence of 3T3-L1 adipocytes was compared (Figure 7B). Although, H_2O_2 production increased in a naphthoquinone-concentration-dependent manner, significantly less H_2O_2 was produced in the presence of 3T3-L1 adipocytes at the same concentration of naphthoquinone ($p < 0.0001$).

Discussion

A prototype four-chamber μCCA device is designed to mimic the complex multitissue (lung, liver, fat, and circulatory system) interactions of living organisms. One of the most important advantages of this device over the other in vitro system is its more physiologically realistic environment. In an earlier prototype, the fabricated multichamber device had suffered from a large hydrodynamic pressure drop (~22 kPa), which led to significant leakage in the system. Through iterative redesign, the pressure drop in the current design is limited to 1 kPa and leaking is negligible, as verified by color dye pumped through the system (Figure 2).

The prior study has demonstrated that the microfluidics in a fabricated four-chamber μCCA device mimics the design of a rat PBPK model reasonably well by comparing the residence time measured in the μCCA device with the actual residence time used in the design calculation (*4*). This finding also suggests that the μCCA system has achieved the desired flow split from the lung chamber to the liver, fat, and other tissue chambers and that the fluid distribution is passively controlled by channel geometries.

We have developed a method to culture three different cell types in their designated compartments and successfully operated the system for at least 6 h. Cells in all compartments remained viable and attach throughout the experiment (Figure 3). Cells on the Matrigel-coated chip exhibited morphologies similar to those particular cells in tissue culture flasks. The L2 cells showed fibroblast-like morphology, while the C3A cell showed more rounded structure, which is the morphology reported for heptocytes growing on the Matrigel matrix in 2D culture (*20*). Moreover, the intracellular lipid in 3T3-L1 adipocytes demonstrates that cells underwent the differentiation process. Thus, we believe that Matrigel provides a suitable environment to support adhesion and differentiation for cells cultured on the μCCA device.

Similar to most of the other microfabricated devices, standard quantification methods at the macroscale, such as HPLC and UV/vis, etc., become difficult, if not impossible, in the μCCA system because of the small liquid volume and the small number of cells to facilitate the analysis (*21*). Moreover, unless fixative is applied, disassembling the device or separating the μCCA chip from the Plexiglas pieces at the end of the experiment can create high hydrodynamic shear on the cells, disrupting the cell layer and potentially altering the results. The alternative measurement approach is fluorescence microscopy. Fluorescence is the most commonly used detec-

tion method in microfluidics (*22*). Measuring fluorescence intensity is sensitive, and fluorescence chemical (fluoranthene) or fluorescence probes (LIVE stain and MCB) are commercially available. Moreover, the fluorescence microscopy allows in situ measurement in micrometer dimension without disturbing the cellular dynamics, which is another advantage of the microfluidic system.

We have studied the bioaccumulation and distribution of fluoranthene in a three-cell, four-chamber μCCA system. Fluoranthene is a product of incomplete combustion and has been identified in air, water, and charbroiled food (*23*). Due to its high hydrophobicity, fluoranthene is likely to absorb to hydrophobic materials, for example poly(dimethylsiloxane) (PDMS) (*24*, *25*), polyacrylate (*26*), or octadecyl-modified silica disk (C18 disks) (*27*), and fluoranthene was detected in the lipid collected from forehead skin of roofing workers (*28*). In the μCCA system, the majority of fluoranthene was found in the fat chamber (Figure 4). Since the fat chamber contains a much larger lipid storage than the other chamber, highly lipophilic fluoranthene preferentially accumulates in this chamber increasing its concentration over time. The level of fluoranthene in the liver was slightly higher than in the lung. Similar to other PAHs, fluoranthene is metabolized by P450 enzyme in the hepatocytes (*29*−*31*), and that may have allowed more fluoranthene to be retained in the liver chamber, where the biotransformation takes place, than in the lung chamber.

The comparison between the two-cell and three-cell μCCA system indicates that the presence of differentiated 3T3-L1 adipocytes reduces naphthalene-induced GSH depletion in both lung (L2) cells and liver (HepG2/C3A) cells (Figure 5). Previously, naphthalene has been shown to accumulate in intracellular lipid of differentiated 3T3-L1 adipocytes (*11*). Although naphthalene was clearly absorbed into the fat compartment in the μCCA system, because of continuous replenishment of naphthalene, the expected level of naphthalene in the fluid should not be altered significantly. The smaller reduction of the GSH level observed in both L2 and C3A cells may be due to sequestration of toxic naphthalene metabolites (e.g., naphthoquinone) in the adipocytes and the byproduct of naphthalene metabolism (i.e., H_2O_2) being reduced in the presence of 3T3-L1 adipocytes. Triglycerides in the adipocytes may act as antioxidants.

Similar to the above finding, the addition of differentiated 3T3-L1 adipocytes to the μCCA system also decreases naphthoquinone-induced GSH depletion in lung (L2) cells (Figure 6A), due to several reasons. First, the partition coefficient of naphthoquinone between adipocytes and medium (690) suggests that naphthoquinone is hydrophobic and would preferentially accumulate into the adipocytes, which can significantly lower the concentration of circulating naphthoquinone in the μCCA system. Naphthoquinone is not replenished in the reservoir as is the case in the naphthalene studies.

One of the possible causes of naphthoquinone toxicity is the reactive oxygen species (ROS), such as O_2^- and H_2O_2, etc., generated from the redox cycle between naphthoquinone and naphthalenediol (*19*). These ROS cause oxidative stress, leading to cellular damage (*32*, *33*). Hydrogen peroxide has been previously identified as one of the possible causes of naphthalene-induced GSH depletion in lung (L2) cells in the two-cell μCCA system (*4*). In the present study, we have shown that significantly less H_2O_2 was observed in the culture medium upon incubation with differentiated 3T3-L1 adipocytes (Figure 7B). It is likely that, because naphthoquinone absorbed into the adipocytes, less naphthoquinone was available to undergo redox cycling and generate H_2O_2, resulting in lower concentration of H_2O_2 present in the medium. The study by Torday et al. (*34*) has suggested the possibility of triglyceride as an antioxidant against reactive oxygen species, including H_2O_2. This observation leads us to speculate that the triglyceride in the adipocytes may have provided a protective effect against H_2O_2. The actual causes of either lower H_2O_2 generation or H_2O_2 disappearance require further investigation. In conclusion, the presence of adipocytes in the μCCA system reduces naphthalene- and naphthoquinone-induced toxicity, possibly from the combination of the accumulation of the naphthoquinone and the disappearance of H_2O_2.

Surprisingly, the level of GSH of C3A cells in the μCCA system did not change significantly upon treatment with naphthoquinone, regardless of the addition of differentiated 3T3-L1 adipocytes. We have shown earlier that liver (C3A) cells are less sensitive toward naphthoquinone than lung (L2) cells, as the level of GSH in C3A cells only decreased slightly compared to that of L2 cells (*4*). Consequently, the C3A cells do not receive much benefit from the presence of 3T3-L1 adipocytes in the μCCA system. Nonetheless, the adipocytes provide a protective effect against toxic compounds, at least those tested here, which is particularly critical for the most sensitive tissue.

Although the differentiated 3T3-L1 adipocytes are a good representation of fat, the utilization of this cell line model in the μCCA device can be somewhat cumbersome. These cells require prolonged incubation time, making the device preparation difficult and lengthy. Some of the differentiated adipocyte cells around the edge started to lift off once flow was introduced into the μCCA system because of the buoyancy force from the lipid component in the cells. To circumvent this problem, other nonliving substrates have been explored to mimic the accumulation of lipophilic compound in adipose tissue. This material is expected to replace the adipocyte cells in the future design of the μCCA device, making the device preparation and operation more practical.

Conclusions

We have demonstrated the application of a four-chamber μCCA system ("lung"−"liver"−"fat"−"other tissue") to study bioaccumulation, distribution, metabolism, and toxicity of the tested compounds. This three-cell system device contains cultures of L2, HepG2/C3A and differentiated 3T3-L1 adipocytes in the lung, liver, and fat chambers, respectively. In the bioaccumulation study, the majority of fluoranthene was observed in the fat chamber. Interestingly, the level of fluoranthene in the liver chamber was slightly higher than in the lung chamber, possibly because of fluoranthene metabolism in the liver. The dynamic response of L2 and C3A cells to naphthalene and naphthoquinone toxicity in the presence of 3T3-L1 adipocytes was also investigated. The addition of differentiated 3T3-L1 adipocytes to the μCCA system reduced naphthalene- and naphthoquinone-induced GSH depletion, due to absorption of these compounds into the intracellular lipid, and the probably reduction of H_2O_2 that causes cellular damage.

A four-chamber μCCA system offers an alternative approach to determine ADMET characteristics of the compound of interest. With some modifications, the future device will be particularly beneficial to pharmaceutical and chemical companies to assess the efficacy and safety of the lead compounds.

Acknowledgment

This work was supported by the Nanobiotechnology Center (NBTC), a STC Program of the National Science Foundation under Agreement No. ECS-9876771, the Cornell Center for Advanced Technology (Biotechnology) with support from the New York State Science and Technology Foundation and a consortium of industries, as well as a matching gift from DuPont, and support from the Faculty Development Program of New York Science, Technology and Academic Research (NYSTAR). This work was performed in part at the Cornell Nanofabrication Facility (a member of the National Nanofabrication Users Network). We would like to thank Greg Baxter and Aaron Sin for helpful discussions and Paula Miller and Glenn Swan for their technical assistance.

References and Notes

(1) Hodgson, J. ADMET-turning chemicals into drugs. *Nat. Biotechnol.* **2001**, *19*, 722−726.

(2) Lee, C.-J.; Lee, L. H.; Lu, C.-H. Drug evaluation from laboratory through licensure to pharmacist's shelf. In *Drug Development and Evaluation of Drugs, from Laboratory through Licensure to Market*, 2nd ed.; CRC Press: New York, 2003; pp 23−116.

(3) Sin, A.; Chin, K. C.; Jamil, M. F.; Kostov, Y.; Rao, G.; Shuler, M. L. The design and fabrication of three-chamber microscale cell culture analogue devices with integrated dissolved oxygen sensor. *Biotechnol. Prog.*, in press.

(4) Viravaidya, K.; Sin, A.; Shuler, M. L. Development of a microscale cell culture analogue to probe naphthalene toxicity. *Biotechnol. Prog.*, in press.

(5) Gerlowski, L. E.; Jain, R. K. Physiological based pharmacokinetics modeling: Principles and applications. *J. Pharm. Sci.* **1983**, *72*, 1103−1127.

(6) Quick, D. J.; Shuler, M. L. Use of in vitro data for construction of a physiologically based pharmacokinetics model for naphthalene in rats and mice to probe species differences. *Biotechnol. Prog.* **1999**, *14*, 540−555.

(7) Anderson, H. A. Utilization of adipose tissue biopsy in characterizing human halogenated hydrocarbon exposure. *Environ. Health Perspect.* **1985**, 60, 127−131.

(8) Ailhaud, G. Development of white adipose tissue and adipocyte differentiation. In *Adipose tissue*; Klaus, S., Ed.; Eurekah.com: Georgetown, TX, 2001; pp 27−54.

(9) Sadowski, H. B.; Wheeler, T. T.; Young, D. A. Gene expression during 3T3-L1 adipocyte differentiation. *J. Biol. Chem.* **1992**, *266*, 4722−4731.

(10) Slieker, L. J.; Sloop, K. W.; Surface, P. L. Differentiation method-dependent expression of leptin in adipocyte cell lines. *Biochem. Biophys. Res. Commun.* **1998**, *251*, 225−229.

(11) Viravaidya, K.; Shuler, M. L. The prediction of naphthalene bioaccumulation using an adipocyte cell line model. *Biotechnol. Prog.* **2002**, *18*, 174−181.

(12) Sin, A. Development of a three-chamber microscale cell culture analogue device. Ph.D. Thesis, Cornell University, Ithaca, NY, August 2002.

(13) Keelan, J.; Allen, N. J.; Antcliffe, D.; Pal, S.; Duchen, M. R. Quantitative imaging of glutathione in hippocampal neurons and glia in culture using monochlorobimane. *J. Neurosci. Res.* **2001**, *66*, 873−884.

(14) Andersen, M. E.; Clewell, H. J., III.; Gargas, M. L.; Smith, F. A.; Reitz, R. H. Physiologically based pharmacokinetics and the risk assessment process for methylene chloride. *Toxicol. Appl. Pharm.* **1987**, *87*, 185−205.

(15) Gearhart, J. M.; Jepson, G. W.; Clewell, J. H.; Andersen, M. E.; Conolly, R. B. Physiologically based pharmacokinetic and pharmacodynamic model for the inhibition of acetylcholinesterase by diisopropylfluorophosphate. *Toxicol. Appl. Pharm.* **1990**, *106*, 295−310.

(16) Dabestani, R.; Ivanov, I. N. A compilation of physical, spectroscopic, and photophysical properties of polycyclic aromatic hydrocarbons. *Photochem. Photobiol.* **1999**, *70*, 10−34.

(17) Bellomo, G.; Palladini, G.; Vairetti, M. Intranuclear distribution, function and fate of glutathione and glutathion-s-conjugate in liver rat hepatocytes studied by fluorescence microscopy. *Microsc. Res. Tech.* **1997**, *36*, 243−252 1997.

(18) Hirsch, J.; Gallian, E. Methods for the determination of adipose cell size in man and animals. *J. Lipid Res.* **1968**, *9*, 110−119.

(19) Bolton, J. L.; Trush, M. A.; Penning, T. M.; Dryhurst, G.; Monks, T. J. Role of quinone in toxicology. *Chem. Res. Toxicol.* **2000**, *13*, 135−160.

(20) Richert, L.; Binda, D.; Hamilton, G.; Viollon-Abadie, C.; Alexandre, E.; Bigot-Lasserre, D.; Bars, R.; Coassolo, P.; LeCluyse, E. Evaluation of the effect of culture configuration on morphology, survival time, antioxidant status and metabolic capacities of cultured rat hepatocytes. *Toxicol. in Vitro* **2002**, *16* (1), 89−99.

(21) Beebe, D.; Mensing, G. A.; Walker, G. M. Physics and application of microfluidics in biology. *Annu. Rev. Biomed. Eng.* **2002**, *4*, 261−286.

(22) Meldrum, D. R.; Holl, M. R. Microfluidics: Microscale bioanalytical systems. *Science* **2002**, *297*, 1197−1198.

(23) IARC (International Agency for Research on Cancer). Fluoranthene. In *IARC monographs on the evaluation of carcinogenic risks to humans. polynuclear aromatic compounds. Part 1. Chemical, environmental and experimental data*; World Health Organization: Lyon, France, 1983; Vol. 32, pp 355−364.

(24) Shurmer, B.; Pawliszyn, J. Determination of distribution constants between a liquid polymeric coating and water by a solid-phase microextraction technique with a flow-through standard water system. *Anal. Chem.* **2000**, *72*, 3660−3664.

(25) Mayer, P.; Vaes, W. H. J.; Hermens, J. L. M. Absorption of hydrophobic compounds into the poly(dimethylsiloxane) coating of solid-phase microextraction fibers: High partition coefficients and fluorescence microscopy images. *Anal. Chem.* **2000**, *72*, 459−464.

(26) Doong, R.; Chang, S. Determination of distribution coefficients of priority polycyclic aromatic hydrocarbons using solid-phase microextraction. *Anal. Chem.* **2000**, *72*, 3647−3652.

(27) Krauss, M.; Wilcke, W. Biomimetic extraction of PAHs and PCBs from soil with octadecyl-modified silica disks to predict their availability to earthworms. *Environ. Sci. Technol.* **2001**, *35*, 3931−3935.

(28) Wolff, M. S.; Taffe, B.; Boesch, R. R.; Selikoff, I. J. Detection of polycyclic aromatic hydrocarbons in skin oil obtained from roofing workers. *Chemosphere* **1982**, *11*, 595−599.

(29) LaVoie, E. J.; Hecht, S. S.; Bedenko, V.; Hoffmann, D. Identification of the mutagenic metabolites of fluoranthene, 2-methylfluoranthene, and 3-methylfluoranthene. *Carcinogenesis* **1982**, *3*, 841−846.

(30) Polcaro, C.; Icoletti, I.; Ossicini, L.; Caponecchi, G. Chromatographic and cytogenetic analysis of *in vivo* metabolites of fluoranthene. *J. Chromatogr.* **1988**, *448*, 127−133.

(31) Babson, J. R.; Russo-Rodriguez, S. E.; Wattley, R. V.; Bergstein, P. L.; Rastetter, W. H.; Liber, H. L.; Andon, B. M.; Thilly, W. G.; Wogan, G. N. Microsomal activation of fluoranthene to mutagenic metabolites. *Toxicol. Appl. Pharmcol.* **1986**, *85* (3), 355−366.

(32) Aust, S. D.; Chignell, C. F.; Bray, T. M.; Kalyanaraman, B.; Mason, R. P. Contemporary issues in toxicology: Free radicals in toxicology. *Toxicol. Appl. Pharmacol.* **1993**, *120*, 168−178.

(33) Palmer, H. J.; Paulson, K. E. Reactive oxygen speicies and natioxidants in signal transduction and gene expression. *Nutr. Rev.* **1997**, *55*, 353−361.

(34) Torday, J. S.; Torday, D. P.; Gutnick, J.; Qin, J.; Rehan, V. Biologic role of fetal lung fibroblast triglycerides as antioxidants. *Pediatr. Res.* **2001**, *49* (6), 843−849.

Accepted for publication October 24, 2003.

BP034238D